Understanding of the experimental concept of radiation absorption of radioactive materials

Soni Prayogi[1]*, Fitria Silviana[2], Zainuddin[3]

[1]Department of Electrical Engineering, Faculty of Industrial Engineering, Pertamina University, Jakarta 12220 Indonesia

[2]Department of Physics Education, Faculty of Mathematics and Natural Sciences, Medan State University, Medan 20221, Indonesia

[3]Department of Physics Education, Faculty of Teacher Training and Education, Syiah Kuala University, Banda Aceh 23111, Indonesia

*Correspondence: soni.prayogi@universitaspertamina.ac.id

Received 9 January 2023, Revised 3 February 2023, Published 27 March 2023

Abstract: In this article, we discuss the experimental absorption of radioactive light radiation on various materials using Geiger Muller. Under certain conditions, Geiger Muller can be used to determine the absorption coefficient of a material. The radioactive rays observed in this experiment are gamma rays. Gamma rays are radioactive rays that have no charge so they cannot be deflected by magnetic or electric fields and have the greatest penetrating power. We made several important results on experimental studies of the absorption of gamma radiation passing through matter. Our results relate to the trend of the unexpected, measured intensity of radiation versus the thickness of the absorber, which confuses students and cannot be explained by many laboratory assistants. Finally, we believe that a distribution function is an effective tool for examining the contribution of the build-up factor in the Geiger Muller calculation of the measured radiation intensity.

Keywords: Geiger Muller, Gamma rays, Build-up, Statistics Poisson

1. Introduction

In the physics education laboratory at Syiah Kuala University, one of the experiments conducted by students focused on studying the exponential decrease of gamma radiation through material detected using a Geiger Muller counter (Bhowmik, 2011). By measuring the intensity of such gamma rays, students can derive linear gamma attenuation coefficients at constant energies in lead and other materials such as aluminum and zinc (Costa & Muleri, 2014). Although the experiment seems simple, systematic deviations from the exponential law occur during the measurement (Susila et al., 2019). As a result, the measured linear attenuation coefficient deviates significantly from the theoretically predicted value (Bahrum et al., 2020). It appears here that the differences observed are caused by photon stacking (Hamdani et al., 2022), a phenomenon well-known among nuclear engineers and medical physicists, but one that is often overlooked in lecture-laboratory experiments.

The intensity (I) of radiation passing through the absorber is expressed by the exponential law, $I = I_0 \exp(-\mu x)$, where I0 is the intensity incident on the tin material (Goiffon et al., 2009), μ is the linear attenuation coefficient at certain energy and x is the thickness of the absorber material (Halim, 2012). In our experiments, the dominant effect that occurs in the attenuation of gamma rays is Compton scattering (El-Amin & Saad, 2017). However, the exponential decline rate assumes that only un-sceptered photons can reach the detector, whereas each Compton scattering event results in a loss of photons (Artiani et al., 2019).

More photons made it through. This is also a problem in high-energy gamma-ray radiation events, due to the Compton effect. Photons do not disappear but are simply scattered by electrons or effects which are like two billiard balls colliding with each other with a loss of energy (Prayogi et al., 2021). As a result, some of the scattered photons can eventually reach the detector outside the tin sheet. This phenomenon is called photon stacking and the factor imposed on the number of photons passing through the barrier is the scattering factor. This factor increases with the thickness of the absorber and is opposite to the exponential decay of the photon

2. Experimental Method

Experiments were carried out using the Geiger Muller detector. The working principle of this detector is that if radiation enters the tube from a radiation source, the radiation will ionize the gas filling. Because there is a voltage difference between the cathode and the anode, an electric field will arise between the two electrodes (Zainuddin et al., 2022). Positive ions (+) will move to the wall of the tube at a relatively slower speed than the electrons moving towards the anode where the speed of motion depends on the given V. With relatively high energy, the electrons will be able to ionize the surrounding atoms, giving rise to electron pairs of secondary ions, tertiary ion pairs, and so on, resulting in a continuous discharge as shown in Figure 1.

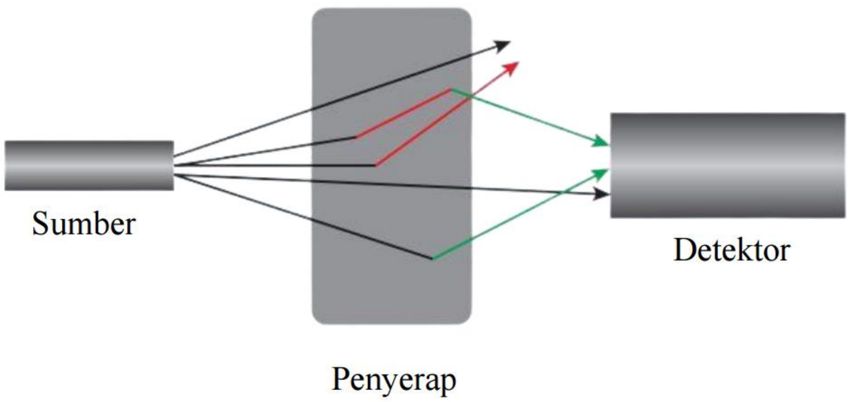

Figure 1. Schematic of the photons emerging from the source (black arrows) can reach the detector without scattering, scatter in different directions, or be scattered away from the detector (red arrows) and towards the detector (green arrows).

J. Phys.: Theor. Appl. Vol. 7 No. 1 (2023) 45-52 doi: 10.20961/jphystheor-appl.v7i1.70138

The gamma rays we use go through a ^{60}Co radioactive source. The ^{60}Co radioactive source emits two gamma rays with energies of 1.173 MeV and 1.325 MeV, which in that energy range interact with matter primarily through Compton scattering. Because there are two different characteristic energies emitted, in our experiments we used a ^{60}Co radioactive source with an energy source of 1.25 MeV. The detector used is a Geiger Muller counter. In the seat between the radioactive source and the detector, we insert an absorbent sheet, which is lead, so it has a linear attenuation coefficient of $\mu = 0.0667$ mm^{-1}.

This experiment was carried out using tools and materials such as a counter which is used to see the output of chopped radioactive sources, the Geiger Muller detector is used as a tool to detect the magnitude of the radiation source coming out of the radioactive source material, the stative is used to clamp the detector which is installed right above the radioactive source with a certain distance, a ruler is used to measure the distance between the detector and the radioactive source, the space holder is used to place the radioactive source which can be varied in the distance, the stopwatch is used to calculate the time of enumeration of the radioactive source as shown in Figure 2.

Figure 2. The equipment and materials used in the experiments

3. A subsection (Subsection style)

The experiment we did was repeated several times. During the measurements, we recorded Geiger Muller numbers for constant time intervals of 2, 3, 4, and 10 minutes. In the first case we use the lower source, the results after subtraction of the background, are given in Table 1.

Table 1. Geiger Muller calculations of five experiments (minus background)

Time interval (minutes)	Lead thickness (mm)	0	3.29	6.50	9.97	13.44	15.10	16.93	18.76
2	Exp 1	121	103	88	72	51	56	68	68
2	Exp 2	156	121	104	96	83	77	72	75
3	Exp 3	223	174	159	133	113	100	101	103
4	Exp 4	294	234	213	174	149	138	141	146
10	Exp 5	750	610	523	445	367	357	332	339

Due to the simple law of exponential attenuation, one would expect that the plot of ln(I) vs x (thickness) is a descending straight line. This was not the case, as in this experiment, which we analyzed can be seen in Figure 3. In experiment 1 (exp 1) the last two points did not show any decrease but on the other hand, the other experiments showed a rapid increase. Similar graphs are produced at exp 2 to exp 5, where more calculations are aggregated across most measurements to reduce statistical error and to clarify the results obtained. It was found that the radiation increased rather than decreased because by using more lead, the detector should have counted less but it did not (Prayogi et al., 2022). Therefore, the detector is not working properly. Even if tried by fitting a straight line through the first four or five trial points on the graph, according to the law of exponential decay mentioned above, the expected value of μ cannot be obtained.

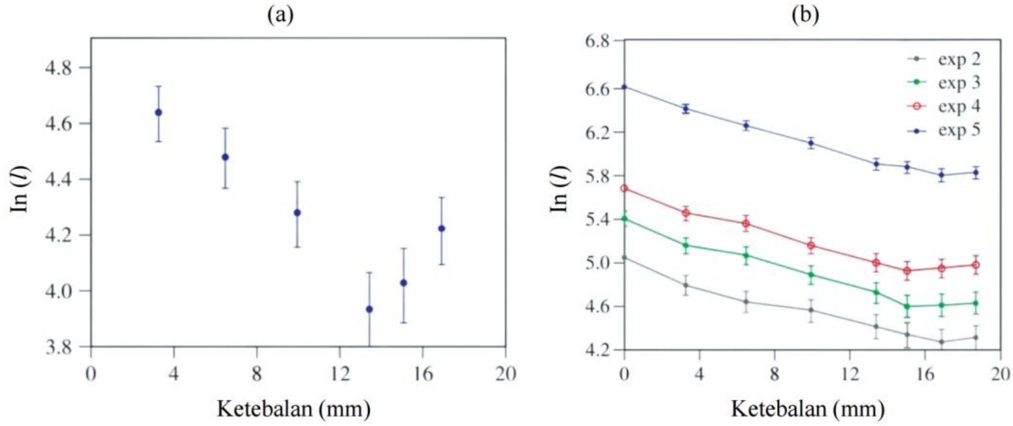

Figure 3. Results of Geiger Muller measurements after subtracting the baground of detected radiation versus lead thickness on a semi-log scale for (a) experiments 1 and (b) experiments 2–5 where a larger source was used

We have tried to investigate this event using the frequency distribution of the quantities recorded for each absorbent thickness. We focus on exp 2, but the conclusions hold on an equal footing to the other experiments. As observed in Figure 4(a), the plot of the frequency of the source radiation recorded by the detector without absorption yielded a single mountain-shaped peak, as expected from radioactive decay Poisson statistics.

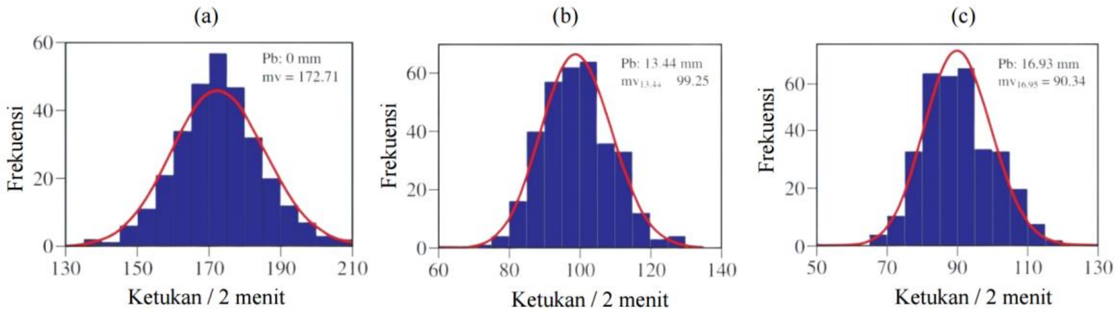

Figure 4. Frequency distribution of calculations for cases (a) without absorbent, (b) with 13.44 mm thick lead absorbent, and (c) with 16.93 mm thick lead absorbent, under experimental conditions 2. The background is not reduced. Theoretical Poisson distribution (red curve) for each experimental mean (mv) value is plotted for comparison

Here we find that this condition also holds for the number of repetitions of measurements made. In contrast, this condition does not occur when the lead is placed between the 60Co source and the detector (see Figure 4(b)). With a 13.44 mm thick lead absorber, the frequency distribution deviates from Poisson and has an increased probability of appearing at higher counts. We believe that with a 13.44 mm thick lead absorber, the frequency distribution deviates from Poisson, and the probability increases at higher counts. The same thing also applies to Figure 4(c).

Table 2. Estimated thickness factor values for ^{60}Co gamma rays through lead

Lead thickness x (mm)	0	3.29	6.50	9.97	13.44	15.10	16.93	18.76
$B(\mu x)$	1.1	1.07	1.16	1.22	1.34	1.39	1.43	1.49

We assume that the weak radiation falling into Poisson statistics is an unerring assumption. Also, because of absorption and consequent lower sums and mean values (mv), the distributions in Figure 4(b) and (c) become much narrower than the Poisson-like distributions in Figure 4(a). In this case, the attenuation measurement to consider the square root of the measured count as the error of the radiation obtained based on our findings, we suggest that such experiments be carried out with caution.

The frequency distribution can also be helpful in explaining the difference in Figure 3 from the law of simple exponential decay by making use of simple calculations. According to the law of exponential decay, we get $\ln(I_2) - \ln(I_1) = -\mu\,(x_2 - x_1)$, where I_i and xi are the intensity and the corresponding thickness values. Then, using the average distribution values in Figures 4(b) and (c) (mv16.93 and mv13.44, where the index corresponds to the tin thickness) corrected for background 25 counts, we obtain $\ln(mv16.93 - 25) - \ln(mv13.44 - 25) = -\mu\,(16.93 - 13.44)$. However, according to this relationship, the linear attenuation coefficient will be obtained as it approaches 0.0366 mm^{-1}, which is much smaller than the value obtained. This reveals that thicker materials can result in additional counts.

The deviation of the frequency distribution of the number of photons measured by the absorber from Poisson statistics is caused by secondary photons, which mainly arise from Compton scattering events from the main beam in absorption reaching the detector (Nicholls et al., 2017). If no stacking effect is obtained and Poisson statistics can be applied, the law of the exponential decrease of radiation through matter will be more easily produced (Kandlakunta et al., 2022). However, because the phenomenon that occurs is a straight-line graph of the logarithm of the incident radiation versus the thickness of the absorber it becomes less clear (as in Figures 2 and 3). Of course, to choose the thicker Pb absorbent sheet to smooth out the extreme irregularities, but again the graph appears as a dotted line, which includes a steep section for small thicknesses and a shallow section for larger absorbent thicknesses.

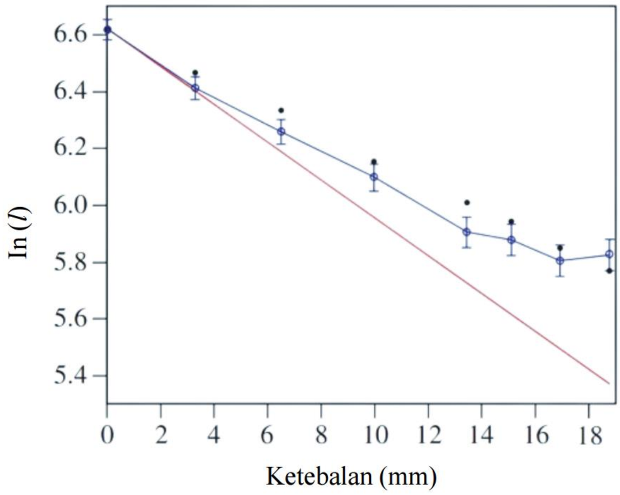

Figure 5. The results of Geiger Muller's calculations in experiment 5 (blue circle) versus the value obtained after adding the stacking factor (black point) and the law of exponential decay (red line).

We have tried to account for the contribution of build-up effects using the simple model $I = B(\mu x)\ [I_0 \exp(-\mu x)]$ for the thickness and intensity values of experiment 5. Here, we use approximate values of the build-up factor (as shown in Table 2) taken from the experimental chart. The intensity values derived by the model equations are plotted in Figure 5, together with the experimental ones and the resulting theoretical exponential decay law (red line). The importance of the corrected value due to the inclusion of the build-up factor is in good agreement with the experimental results (Prayogi et al., 2022). More accurate build-up factors can be used but are only available at cost from the American Nuclear Society. It is proved that the experimental setup and model equations can be used for the study of gamma-ray attenuation and photon stacking in the laboratory.

4. Conclusion

In conclusion, this investigation underscores that while the distribution function (frequency versus Geiger Muller measurement) for the decay of a radioactive source is well described by Poisson statistics, this is not the case when an absorber is present. In this case, because of the build-up factor, the distribution function assumes a distorted width structure to a higher value than it produces and makes applying simple Poissonian statistics an approximation. This results in (i) larger errors in the Geiger Muller measurements, (ii) larger errors in the linear attenuation coefficients, and (iii) a systematic decrease in the average value of the attenuation coefficients. Finally, we believe that a distribution function is an effective tool for examining the contribution of the build-up factor in the Geiger Muller calculation of the measured radiation intensity. This experimental device, although impractical, can be used to investigate radioactive rays very effectively. As build-up factors depend on the nature, construction, and strength of the radioactive source, absorbent material, thickness, and geometry as well as the presence of shielding relative spacing between various parts of the arrangement and other factors.

Acknowledgments

The authors thank Pertamina University and Syiah Kuala University for the support and facilities that have been provided

References

Artiani, P.A., Ratiko, R., Purwanto, Y., & Heriyanto, K., (2019). Pengaruh Perisai Radiasi Pada Penyimpanan Kering Bahan Bakar Nuklir Bekas untuk Reaktor Daya Eksperimental. Jurnal Pengembangan Energi Nuklir 20, 83–93. https://doi.org/10.17146/jpen.2018.20.2.5025

Bahrum, E.S., Handiaga, W., Setiadi, Y., Wibowo, H., Basuki, P., Maulana, A., Febrian, M.B., & Pane, J.S., (2020). DESIGN OF IRRADIATION FACILITIES AT CENTRAL IRRADIATION POSITION OF PLATE TYPE RESEARCH REACTOR BANDUNG. JURNAL TEKNOLOGI REAKTOR NUKLIR TRI DASA MEGA 22, 1–8. https://doi.org/10.17146/tdm.2020.22.1.5762

Bhowmik, S., (2011). Effect of Radiation and Vacuum, in: da Silva, L.F.M., Öchsner, A., Adams, R.D. (Eds.), Handbook of Adhesion Technology. Springer, Berlin, Heidelberg, pp. 823–844. https://doi.org/10.1007/978-3-642-01169-6_32

Costa, E., & Muleri, F., (2014). Gamma and X-Radiation, in: Njoku, E.G. (Ed.), Encyclopedia of Remote Sensing, Encyclopedia of Earth Sciences Series. Springer, New York, NY, pp. 219–228. https://doi.org/10.1007/978-0-387-36699-9_49

El-Amin, A.A., & Saad, M.H., (2017). Ionizing Radiations (Alpha, Beta, Gamma) Effects on CdS / P-Si Heterojunction Solar Cell for Electrical and Optical Properties. Journal of Materials Science Research 7, p20. https://doi.org/10.5539/jmsr.v7n1p20

Goiffon, V., Magnan, P., Saint-Pé, O., Bernard, F., & Rolland, G., (2009). Ionization versus displacement damage effects in proton irradiated CMOS sensors manufactured in deep submicron process. Nuclear Instruments and Methods in Physics Research Section A: Accelerators, Spectrometers, Detectors and Associated Equipment, New Developments In Photodetection NDIP08 610, 225–229. https://doi.org/10.1016/j.nima.2009.05.078

Halim, M.A., (2012). Harnessing Sun's Energy with Quantum Dots Based Next Generation Solar Cell. Nanomaterials (Basel) 3, 22–47. https://doi.org/10.3390/nano3010022

Hamdani, D., Prayogi, S., Cahyono, Y., Yudoyono, G., & Darminto, D., 2022. The influences of the front work function and intrinsic bilayer (i1, i2) on p-i-n based amorphous silicon solar cell's performances: A numerical study. Cogent Engineering 9, 2110726. https://doi.org/10.1080/23311916.2022.2110726

Kandlakunta, P., Van Zile, M., & Cao, L.R., (2022). Silicon Solar Cells for Post-Detonation Monitoring and Gamma-Radiation Effects. Nuclear Science and Engineering 196, 1383–1396. https://doi.org/10.1080/00295639.2022.2091905

Nicholls, D.C., Dopita, M.A., Sutherland, R.S., & Kewley, L.J., (2017). Chapter 17 - Electron Kappa Distributions in Astrophysical Nebulae, in: Livadiotis, G. (Ed.), Kappa Distributions. Elsevier, pp. 633–655. https://doi.org/10.1016/B978-0-12-

804638-8.00017-6

Prayogi, S., Asih, R., Priyanto, B., Baqiya, M.A., Naradipa, M.A., Cahyono, Y., & Darminto, Rusydi, A., (2022). Observation of resonant exciton and correlated plasmon yielding correlated plexciton in amorphous silicon with various hydrogen content. Sci Rep 12, 21497. https://doi.org/10.1038/s41598-022-24713-5

Prayogi, S., Cahyono, Y., & Darminto, D., (2022). Electronic structure analysis of a-Si: H p-i1-i2-n solar cells using ellipsometry spectroscopy. Opt Quant Electron 54, 732. https://doi.org/10.1007/s11082-022-04044-5

Prayogi, S., Cahyono, Y., Iqballudin, I., Stchakovsky, M., & Darminto, D., (2021). The effect of adding an active layer to the structure of a-Si: H solar cells on the efficiency using RF-PECVD. J Mater Sci: Mater Electron 32, 7609–7618. https://doi.org/10.1007/s10854-021-05477-6

Susila, I.P., Alfiansyah, A., Istofa, I., Sukandar, S., Santoso, B., & Suratman, S., (2019). DEVELOPMENT OF MOBILE DEVICE FOR GAMMA RADIATION MEASUREMENT UTILIZING LORA AS THE COMMUNICATION MEANS. JURNAL TEKNOLOGI REAKTOR NUKLIR TRI DASA MEGA 21, 79–86. https://doi.org/10.17146/tdm.2019.21.2.5432

Zainuddin, Z., Syukri, M., Prayogi, S., & Luthfia, S., (2022). Implementation of Engineering Everywhere in Physics LKPD Based on STEM Approach to Improve Science Process Skills. Jurnal Pendidikan Sains Indonesia (Indonesian Journal of Science Education) 10, 231–239. https://doi.org/10.24815/jpsi.v10i2.23130